EurJOC
European Journal of Organic Chemistry

A Journal of
ChemPubSoc Europe

Accepted Article

Title: Synthesis, Properties, and Functionalization of Non-symmetric 8-MethylthioBODIPYs

Authors: Jorge Bañuelos; Antonio Gómez-Infante; Ismael Valois-Escamilla; David Cruz-Cruz; Ruth Prieto-Montero; Iñigo Lopez-Arbeloa; Teresa Arbeloa; Eduardo Peña-Cabrera

To be cited as: Eur. J. Org. Chem. 10.1002/ejoc.201600724

Link to VoR: http://dx.doi.org/10.1002/ejoc.201600724

Supported by
ACES Asian Chemical Editorial Society

WILEY-VCH

FULL PAPER WILEY-VCH

Synthesis, Properties, and Functionalization of Non-symmetric 8-MethylthioBODIPYs

Antonio de J. Gómez-Infante,[a] Jorge Bañuelos,*[b] Ismael Valois-Escamilla,[a] David Cruz-Cruz,[a] Ruth Prieto-Montero,[b] Iñigo López-Arbeloa,[b] Teresa Arbeloa[b] and Eduardo Peña-Cabrera,*[a]

Abstract: Five new non-symmetric BODIPY dyes based on the Biellmann´s methodology (NSBB) were prepared by the condensation reaction of two different pyrroles with thiophosgene. Treatment of the resulting thioketones with MeI and $BF_3{\cdot}Et_2O$/TEA yielded a wide battery of products in a simple manner, with selective alkylation of each pyrrole of the indacene core and with a controlled functionalization at the *meso* position. A comprehensive combined photophysical and computational study have been conducted to settle the impact of the alkylation pattern, as well as the role of the conformational freedom and electron coupling of the 8-phenyl and 8-methylthio groups on the spectroscopic signatures of BODIPYs. The results and conclusions reached are compared with previously reported related analogs. We intend to provide key structural guidelines which trigger the fluorescence response as well as the spectral shifts of this family of multifunctional fluorophores.

Introduction

In the last few decades, borondipyrromethenes (BODIPYs) **1**, have established themselves as some of the most versatile fluorophores. A number of review papers have documented their synthesis, properties, and applications.[1]

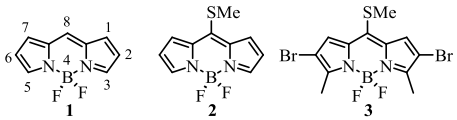

1 **2** **3**

Likewise, Biellmann and co-workers described in 2007 the synthesis, characterization, and preliminary reactivity of 8-methylthioBODIPY (henceforth called Biellmann BODIPY) **2**.[2] Following this publication, our group has demonstrated the synthetic versatility of **2** and that of a more functionalized version, **3**. For example, **2** efficiently participates in the so-called Liebeskind-Srogl cross-coupling reaction (LSCC)[3] with both boronic acids and organostannanes,[4] also in S_NAr-like reactions that allow for the displacement of the MeS- group by amines,[5] thiols,[6] alcohols and phenols,[7] stabilized nucleophiles,[8] and phosphines[9] (Scheme 1).

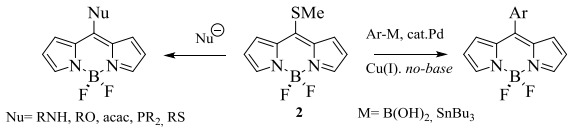

Scheme 1. Typical transformations of Biellmann BODIPY **1**

Similarly, we have demonstrated that **3** displays orthogonal reactivity[10] allowing completely chemoselective sequential reactions at the 8-position (LSCC and S_NAr), 3- and 5-methyl groups (Knoevenagel) and Suzuki, Stille, and Sonogashira reactions at the 2- and 6-positions (Scheme 2).

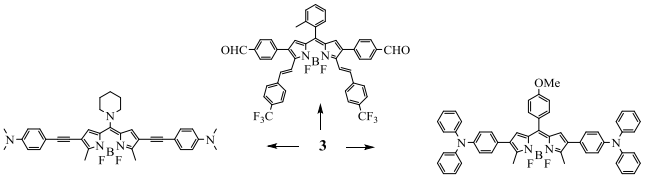

Scheme 2. Examples of products that can be prepared from **3.**

Given the privileged structure of **2** and **3**, it would be desirable to prepare analogues that would permit a more diverse series of reactions. Thus, and taking these scaffolds as starting points, we have preliminary evaluated the reactivity of a series of non-symmetrical Biellmann BODIPYs (NSBB), with selective and specific functionalization of the dipyrrin core. The developed set of multifunctional compounds allows a systematic study of the stereoelectronic effect of the alkylation on the dipyrrin core, as well as of the type of substituent at the *meso* position (from sulphur to phenyl or hydrogen). The photophysical and computation characterization of these fluorophores enable to get deeper insight into the role of the molecular structure on the spectroscopic signatures of these dyes. To this aim, related BODIPYs (with symmetric substitution pattern) commercially

[a] Dpto. Química
Universidad de Guanajuato
Col. Noria Alta S/N, 36050 Guanajuato (Mexico)
E-mail: eduardop@ugto.mx
[b] Dpto.Química Física
Universidad del País Vasco (UPV/EHU)
Aptdo. 644, 48080, Bilbao (Spain)
E-mail: jorge.banuelos@ehu.es
http://www.ehu.eus/especmolecular/

Supporting information for this article is given via a link at the end of the document.

available or previously reported in the literature have been also considered. Taking into account that these dyes are the cornerstone of a multitude and increasing number of research contributions, the understanding of such structure-photophysics relationship is a key issue,[11] which would shed light into the prediction of novel tailor made BODIPYs for the target application. Moreover, by breaking the usual plane of symmetry of most BODIPYs (perpendicular to the BODIPY plane), one can envision the possibility to prepare BODIPYs with torsional chirality starting with the NSBBs and introducing non-symmetric, non-rotating substituents at the *meso*-position. BODIPYs with chiral axis of symmetry have attracted significant attention in recent years.[12] Likewise, NSBB hint at the possibility of having a pyrrole half fully blocked and the other half fully open for preparing dimers with potentially interesting properties.[13]

Results and Discussion

Synthesis

Table 1. Synthesis of non-symmetric dipyrrylthioketones

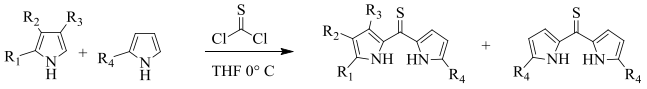

4: R_1=R_3=Me, R_2=H
5: R_4=H
6: R_1=R_3=Me, R_2=Et
7: R_4=Me

8: R_1=R_3=Me, R_2=R_4=H
9: R_1=R_3=R_4=Me, R_2=H
10: R_1=R_3=Me, R_2=Et, R_4=H
11: R_1=R_3=R_4=Me, R_2=Et
12: R_1=Me, R_2=R_3=R_4=H

13: R_4=H
14: R_4=Me

Entry	Mole ratio of pyrroles		Product	Yield[a] (%)	Product ratio[b]
	 **4**	 **5**			
1	1	2	**8**	32	**8/13**=3/1
2	2	1		72	**8/13**=4/1
	 **4**	 **7**			
3	1	2	**9**	13	**9/14**=1/1
4	2	1		14	**9/14**=3/1
	 **6**	 **5**			
5	1	2	**10**	21	**10/13**=1/1
6	2	1		45	**10/13**=8/1
	 **6**	 **7**			
7	1	2	**11**	0	Only **14** was observed
8	2	1		22	**11/14**=3/1
	 **7**	 **5**			
9	1	2	**12**	-[c]	-[c]
10	2	1		-[c]	-[c]

[a] Isolated yield. [b] Determined after the purification of the individual thioketones. [c] The thioketones gave an inseparable mixture that made very difficult both the estimation of their ratio and their purification. However, the mixture was separated once the thioketone mixture was converted to the methylthioBODIPYs (vide infra).

The synthetic methodology used was based on the original report by Biellmann for the synthesis of symmetric **2**,[2] i.e., reaction of two equivalents of pyrrole with thiophosgene, followed by S-methylation with MeI, and finally, treatment with $BF_3.OEt_2$ in the presence of triethylamine. First, the dipyrrylthioketones were prepared according to Table 1. To this end, the stoichiometry of the different substituted pyrroles was varied so that the formation of the crossed products would be favored. Despite the fact that mixtures were obtained in all of the experiments, the separation of the components in the crude materials was manageable, except for thioketones **12**/**13**. In no case, however, the symmetric thioketones that would arise from the more highly substituted pyrroles (**4**, **6**, and **7**) were obtained, presumably, due to steric factors. From the results obtained, it is apparent that, in order to favor the crossed product, the more electron-rich pyrrole has to be in excess. The reaction of **5** and **7** with thiophosgene gave an inseparable mixture of **12** and **13**, which was carried over to the next step, thioketone **14** was not observed. Once the **12**/**13** mixture was converted to the corresponding BODIPYs, it was easily separated.

Once the dipyrrylthioketones were so obtained, the synthesis of the NSBB followed as shown in Table 2.

Table 2. Synthesis of NSBBs[a]

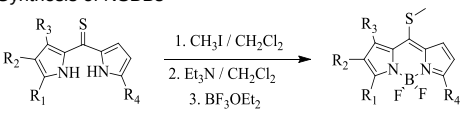

Entry	Dipyrrylthioketone	NSBB/% yield[b]
1	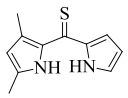 **8**	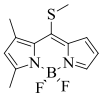 **15,** 63%
2	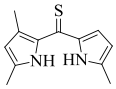 **9**	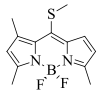 **16**, 36%
3	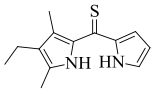 **10**	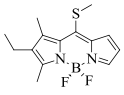 **17**, 29%
4	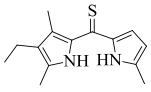 **11**	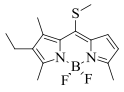 **18**, 32%
5	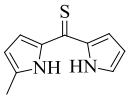 **12**	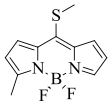 **19**, 27%[c]

[a] Conditions: Thioketone (1.0 equiv), MeI (5.0 equiv), then TEA (1.4 equiv), $BF_3.OEt_2$ (1.4 equiv). [b] Overall isolated yields. [c] Overall from the initial pyrroles.

The two-step sequence to prepare **15**-**19** was somewhat inefficient for the NSBB were obtained in modest to poor yields. There was no evident correlation between either the steric or electronic features of the dipyrrylthioketones **8**-**12** with the observed yields. However, the sequence was efficient enough to prepare the NSBBs in preparative amounts.

It was then decided to preliminary evaluate their reactivity both in the LSCC and the desulfitative reduction.[14]

In a model study, BODIPYs **15**-**19** were reacted with phenylboronic acid under the typical LSCC conditions. The results are illustrated in Table 3.

Table 3. Reactivity of the NSBBs in the LSCC reaction.[a]

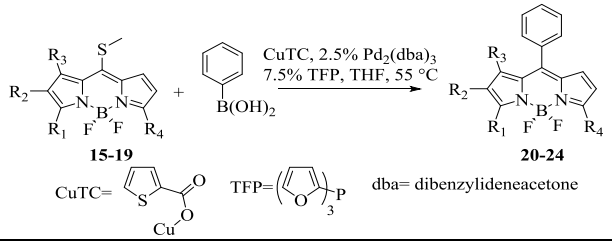

Entry	NSBB	Reaction time (h)	Product/% yield[b]
1	**15**	1.25	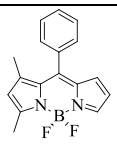 **20**, 50%
2	**16**	1.50	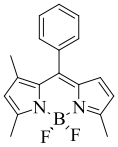 **21**, 58%
3	**17**	1.00	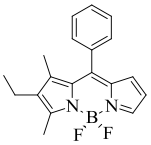 **22**, 75%
4	**18**	1.25	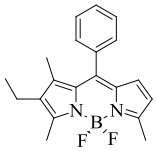 **23**, 60%
5	**19**	1.5	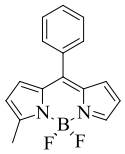 **24**, 81%

[a] Conditions: NSBB (1 equiv), phenylboronic acid (3 equiv), CuTC (3 equiv), $Pd_2(dba)_3$ (2.5%), TFP (7.5%), THF, 55 °C. [b] Isolated yields

The LSCC reaction of **15**-**19** with phenylboronic acid was carried out in a straightforward manner with reaction times comparable to those observed for **2** (1.0-1.5 h).[4a] The overall yields were somewhat diminished when there was a methyl group at the 1-position of the BODIPY core, presumably due to steric hindrance (entries 1-4). BODIPY **24**, lacking a substituent at the 1-position, gave the highest yield (81%, entry 5).

Next, the desulfitative reduction of NSBBs 15-19 was studied (Table 4).

Table 4. Desulfitative reduction of **15**-**19**.[a]

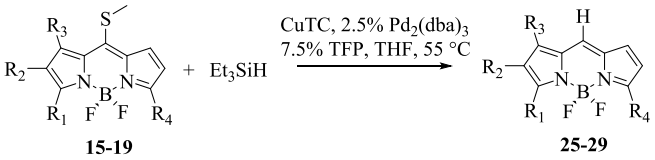

Entry	NSBB	Reaction time (h)	Product/% yield[b]
1	**15**	1.25	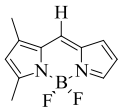 **25**, 89%
2	**16**	1.00	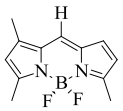 **26**, 91%
3	**17**	1.00	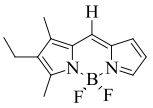 **27**, 90%
4	**18**	1.00	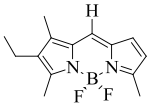 **28**, 70%
5	**19**	1.00	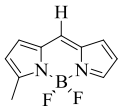 **29**, 90%

[a] Conditions: NSBB (1 equiv), triethylsilane (3 equiv), CuTC (3 equiv), $Pd_2(dba)_3$ (2.5%), TFP (7.5%), THF, 55 °C. [b] Isolated yields

Good to excellent yields were observed in all cases (70-91%) of this clean reaction after 1 h. Both, the yield and the reaction time were very similar to those observed for the same reaction on BODIPY **2**.[14]

Finally, in order to demonstrate the introduction of an additional reaction site, **15** was brominated to give multifunctional BODIPY **30** (eq. 1). Interestingly, the bromination took place exclusively (79%) on the more electron-rich pyrrole ring, rather than in the more accessible one.

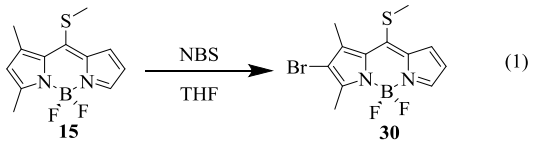

(1)

Spectroscopic Properties

Alkylated BODIPYs. The photophysical properties of the set of non-symmetric compounds shown in Table 4 are gathered in Table 5 and the corresponding spectra in Figure S1 in ESI. As a common rule, the attachment of the inductive electron-donor methyl groups to a conjugated framework should lead to a progressive and accumulative bathochromic shift. Nevertheless, in BODIPYs the magnitude and direction of the spectral band shift promoted by the alkylation depends on the position of the alkyl groups in the chromophore. On one hand, the substitution at the α- (see compounds **29** and **31** *vs* the reference **1**, **26** *vs* **25**, and **28** *vs* **27**, in Table 5) and β-pyrrolic positions (**27** *vs* **25**, and PM567 *vs* PM546 in Table 5) provide the expected bathochromic shift. Especially meaningful is the symmetric substitution at the former 3 and 5 positions (beginning and end of the cyanine-like delocalized π-system) in compound **31**, which not only causes a high bathchromic shift (around 10 nm), but also clearly increases the light absorption probability (molar absorption from 67000 M^{-1} cm^{-1} in dye **1** to 111000 M^{-1} cm^{-1} in compound **26**, in Table 5). On the other hand, the methylation at positions 1 and 7, or 8, promotes the opposite trend, and a slight hypsochromic shift is observed (compound **25** *vs* **29** upon methylation at position 1, or PM546 vs BODIPY 505/515 upon *meso*-methylation, Table 5).

Table 5. Photophysical properties of the alkylated BODIPYs (both non-symmetrical herein synthesized, and symmetrical for comparison, see footnote) in diluted solutions of tetrahydrofuran (2μM); absorption (λ_{ab}) and fluorescence (λ_{fl}) wavelength, molar absorption (ε_{max}), fluorescence quantum yield (ϕ) and lifetime (τ), radiative (k_{fl}) and non-radiative (k_{nr}) rate constants.

Cmpd	Structure	λ_{ab} (nm)	$\varepsilon_{max}\cdot10^{-4}$ (M^{-1} cm^{-1})	λ_{fl} (nm)	ϕ	τ (ns)	k_{fl} (10^8 s^{-1})	k_{nr} (10^8 s^{-1})
1	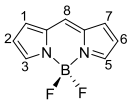	500.0	6.7	506.5	0.84	6.50	1.29	0.25
29	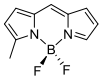	501.5	5.2	509.0	0.82	6.26	1.31	0.29
31	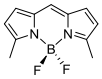	508.5	10.1	515.0	0.86	5.73	1.50	0.25
25	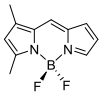	496.0	4.5	505.0	0.84	5.77	1.46	0.28
26	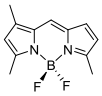	506.0	11.1	511.0	0.89	6.26	1.46	0.18
BODIPY 505/515	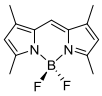	505.5	11.8	511.0	0.82	5.27	1.56	0.34
PM546	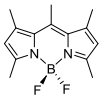	504.0	9.3	509.0	0.85	5.35	1.53	0.40
27	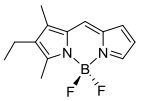	506.5	2.8	517.0	0.79	5.19	1.53	0.40
28	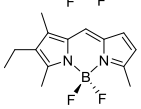	517.0	5.7	524.0	0.89	5.75	1.55	0.19
PM567	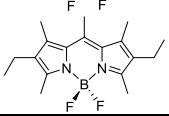	519.0	8.8	538.0	0.84	5.95	1.41	0.27

PM546, PM567 and BODIPY 505/515 are commercially available (see experimental section), whereas compounds **1** and **31** have been previously published by us.[9]

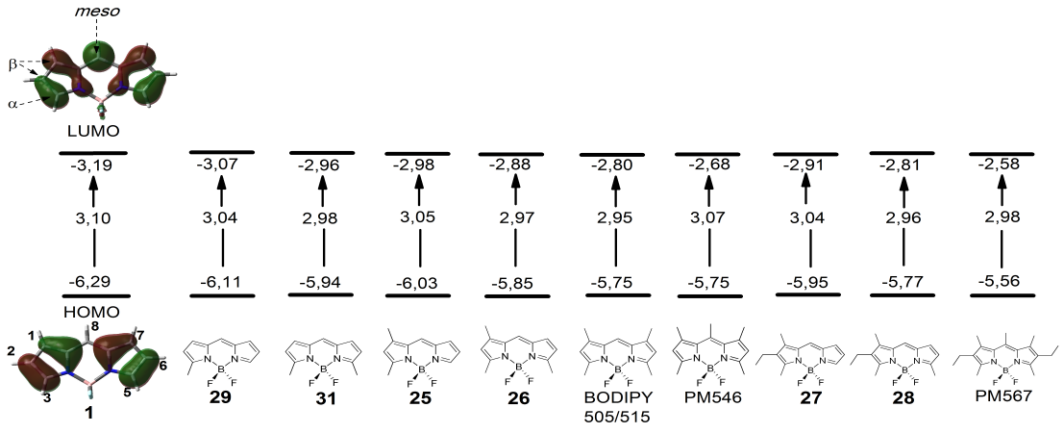

Figure 1. HOMO and LUMO energies (eV) of alkyl-BODIPYs. The corresponding contour maps of the simplest compound **1** are included for a better rationalization of the alkylation effect.

These spectral evolutions with regard to the alkylation pattern can be rationalized qualitatively with the help of the energies corresponding to the frontier orbitals involved in the electronic transition (HOMO and LUMO in Figure 1), even though the spectral shifts are quite low in some cases. At a first sight, the electronic density at positions 3 and 5 is similar in both orbitals, so no preferred stabilization altering the energy gap should be expected. However, a clear bathochromic shift is recorded owing to an increase in the HOMO energy. This is assigned to the push-pull effect promoted by the substitution at these α-pirrolic positions, which enhances the delocalization along the dipyrrin core.[15] In the rest of the chromophoric positions the electronic density clearly changes between both frontier orbitals, mainly in the meso one where the HOMO shows a node. On one hand, the LUMO state shows more electronic density at positions 1, 7 and 8. Thus, the inductive effect of the alkyl groups at those positions promotes an increase of the LUMO energy and thereby enhances the energy gap (Figure 1), in agreement with the hypsochromic shift registered for **25** *vs* **29** (substitution at position 1) or BDP505/510 *vs* PM546 (at *meso* position, Table 5). On the other hand, the HOMO shows higher electronic density at positions 2 and 6. Thus, the alkylation increases the HOMO energy and hence decreases the energy gap (Figure 1), in concordance with the bathochromic shift registered for **27** *vs* **25** or PM567 *vs* PM546 (Table 5). An increase of the aromaticity between the pyrrole rings has been also pointed out to account for such spectral shift upon substitution with electron donating groups at these last β-positions.[16]

Another remarkable issue is the asymmetry/symmetry of the alkylation pattern. Thus, compound **27** (with just one pyrrole fully alkylated) shows the lowest molar absorption (28000 M^{-1} cm^{-1} in Table 5). Indeed, this value progressively increases as both pyrroles are simultaneously and symmetrically alkylated (i.e., from compound **28** to PM567). Furthermore, compound **27** is the BODIPY with the lowest fluorescence quantum yield (79%) and fastest lifetime (5.19 ns). This could be ascribed to a non-symmetric charge distribution between the pyrrole rings. Such charge separation reduces the electronic aromaticity and increases the non-radiative deactivation probability (compound **27** shows the higher k_{nr} in Table 5).[17] The rest of the alkylated dyes show strong and bright fluorescence with values approaching the 90 % (Table 5), and should behave well as laser dyes or fluorescence probes. This is not strange since the geometry remains nearly planar and rigid upon excitation (see Figure S2 in ESI). In fact, the short Stokes shift (< 600 cm^{-1}), suggest very low geometrical rearrangement in the excited state, and hence low internal conversion deactivation. Just slight deviations from planarity (up to 5º in the indacene core) are predicted upon substitution at positions 2 and 6 owing to the generated steric hindrance with the adjacent substituents,[16] which leads to a slight butterfly-like distortion in compound **27**, **28** and PM567 (Figure S2 in ESI).

8-Phenyl-BODIPYs. The role of the 8-aryl in the photophysical signatures of the BODIPY core has been described in the literature.[18] Such reports overall deal with BODIPYs where the 8-aryl rotational motion was fully unconstrained (no substitution at the adjacent positions,) or strongly hampered (via methylation at chromophoric positions 1 and 7, or alternatively by substitution at the *ortho* position of the phenyl group).[19]

In brief, arylation at *meso* position has little impact in the spectral band positions, but its free motion enables non-radiative relaxation pathways and a feasible electron coupling between the *meso*-phenyl and the indacene core upon photoexcitation.[18] Thus, unconstrained 8-phenyl-BODIPYs (i.e., compound **32** with a twisting angle for the phenyl of 56º in S_0 and 47º in S_1, see Figure S3 in ESI) are characterized by low fluorescence efficiency (lower than 3%, see compound **32** in Table 6). This quenching can be avoided by inducing steric hindrance against the 8-phenyl motion to block it in an orthogonal arrangement (twisting angle 90º both in S_0 and S_1, for compound **34**, Figure S3 in ESI), leading to a recovery of the fluorescence response (up to 56% for dye **34** in Table 6).[19]

Table 6. Photophysical properties of the non-symmetric 8-phenyl-BODIPYs in diluted solutions of tetrahydrofuran (2μM). For the sake of comparison, the corresponding data reported in the bibliography for the unsubstituted reference compound 324b and the symmetrically alkylated compounds (**33**[20] and **34**[21]) have been included. The calculated rotational barriers (E_{rot}) for the 8-phenyl in the ground state are also added.

Cmpd	Structure	λ_{ab} (nm)	$\varepsilon_{max}\cdot10^{-4}$ (M^{-1} cm^{-1})	λ_{fl} (nm)	ϕ	$\tau^{[a]}$ (ns)	k_{fl} (10^8 s^{-1})	k_{nr} (10^8 s^{-1})	E_{rot} (kcal mol^{-1})
32	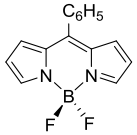	499.0	6.0	518.0	0.023	0.26	0.88	49.8	11.3
24	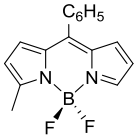	503.5	6.2	520.5	0.039	0.30	1.30	32.0	12.6
33	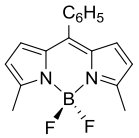	510.0	-	525.0	0.25	1.71	1.46	4.38	12.5
20	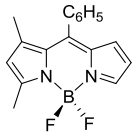	498.0	4.7	514.0	0.022	0.08	2.75	122.2	16.3
21	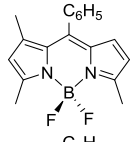	504.0	9.0	517.0	0.020	0.11	1.82	89.1	17.0
34	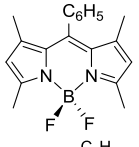	500.0	-	510.0	0.56	3.06	1.83	1.44	26.4
22	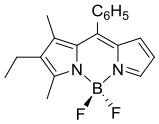	510.0	4.7	528.0	0.022	0.09	2.44	108.6	16.9
23	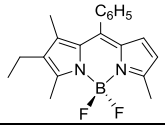	515.0	8.4	530.5	0.020	0.14	1.42	70.0	17.2

[a] Just the main lifetime (contribution > 97%) of the biexponential fit is provided. The second lifetime was around 2-3 ns with minor contribution (down to 2%).

The molar absorptions of **33** and **34** were not provided in the bibliography.

Against this background, the herein reported non-symmetric BODIPYs (**20**-**24**, Table 3) seem ideal to get deeper insight into the effect of the 8-phenyl free motion by controlled increase of the geometrical constrains (i.e., substitution in just one neighbor position). The spectral band positions (Figure S4 in ESI) are similar to their corresponding non-arylated counterparts (Table 6 *vs* Table 5). Strikingly, the fluorescence efficiency remains low in all of them, in spite of the attachment of just one methyl at position 1 (Table 6). Moreover, the α–methylation in the non-symmetric BODIPYs (**20**-**24**) neither ameliorates the fluorescence response, whereas the symmetric derivative bearing methyl groups at such positions (compound **33**)[20] provided improved fluorescence efficiency (Table 6), accordingly to the aforementioned push-pull effect.[4b,15] Such apparent mismatch can be explained by the non-symmetric alkylation pattern, which enhances the non-radiative deactivation and counteracts the beneficial effect of the α-susbtitution.[17] Nevertheless, one should expect a recovery of the fluorescence signal for compounds **20**-**23** owing to the steric hindrance exerted by the adjacent methyl at position 1 against the 8-phenyl rotational freedom. Indeed, the twisting angle increases from 56º for compound **24** to 73º for compound **20** in S_0, but again decrease upon excitation (55º for **20** in S_1, Figure S3 in ESI). Such planarity loss upon excitation in compounds **20**-**23**)

anticipates the tendency of the 8-aryl to distort the chromophore upon excitation. Indeed, the methylation at the adjacent position 1 increases the rotational barrier (from 12 kcal/mol in the unconstrained compound **32** to 17 kcal/mol in **20**, Figure 2) but it is not enough to avoid the deleterious effect of the 8-aryl motion in the fluorescence response (Table 6). To completely suppress such negative influence more constrained geometries are required (such as **34,** barrier around 26 kcal/mol, Figure 2) and fix the 8-phenyl in an orthogonal arrangement (fluorescence efficiency increase from around 2% in compounds **20**-**23** to 56% in **34**, Table 6).

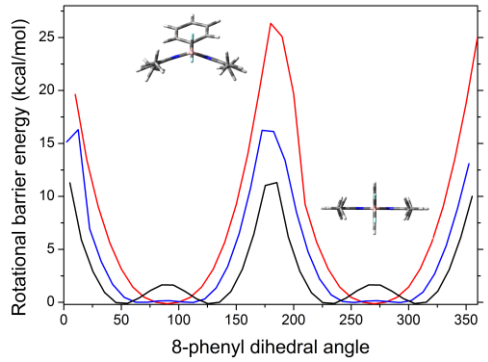

Figure 2. Ground state potential energy surface for the rotation of the phenyl at meso position of the indacene core for the reference compound **32** (black) and its 5,7-dimethylated (**20**, blue) and 1,3,5,7-tetramethylated (**34**, red) derivatives. The corresponding stable and unstable geometries of the last compound are also provided.

Therefore, strong steric hindrance is needed to recover a bright fluorescence signal in 8-arylated BODIPYs. In this regard the methylation at just one adjacent position does not provide the enough steric hindrance. It is true that the coplanar disposition available at the excited is likely more hindered and that the most stable conformation is more twisted, but the distortion of the indacene planarity upon photoexcitation still seems to take place. Thus, in compounds **20**-**23**, the 8-phenyl fragment retains enough rotational freedom. In this regard, the ortho-substitution of the aryl group is more efficient because the ring bears such steric hindrance along the whole rotational movement, increasing the rotational barrier (up to 35 kcal/mol).[4b]

8-Methylthio-BODIPYs. The presence of heteroatoms at *meso* position entails remarkable changes in the spectroscopic signatures of the BODIPY, which can be modulated in term of their electronegativity.[9] In this section, in particular we will focus on the influence of the 8-methylthio group. Such group (compound **2**) should lead to a spectral bathochromic shift with regard to the reference compound **1** owing to the LUMO stabilization caused by the inductive electron withdrawing character of the sulphur atom. Nonetheless, the feasible electronic coupling of the methylthio group with the indacene core provides an alternative delocalized π–system (Figure 3).[9]

As a consequence, the absorption spectrum comprises two bands (or shoulders, depending on the alkylation of the dipyrrin core, as will be discussed later) corresponding to the stabilization of each mesomeric form; the long-wavelength band from the cyanine-like delocalization expected for BODIPYs, and the short-wavelength band, which results from the selective electronic coupling of the methylthio group with one chomophoric pyrrole (Figure 3). In contrast, the shape of the fluorescence spectra of dye **2** fully resembles that recorded for BODIPYs, but bathochromically shifted with regard to the unsubstituted compound **1**, owing to the expected and aforementioned lowering of the energy gap by the 8-methylthio moiety (Table 7). Therefore, the contribution of the new resonance structure takes place mainly in the ground state, whereas upon excitation the cyanine one prevails.

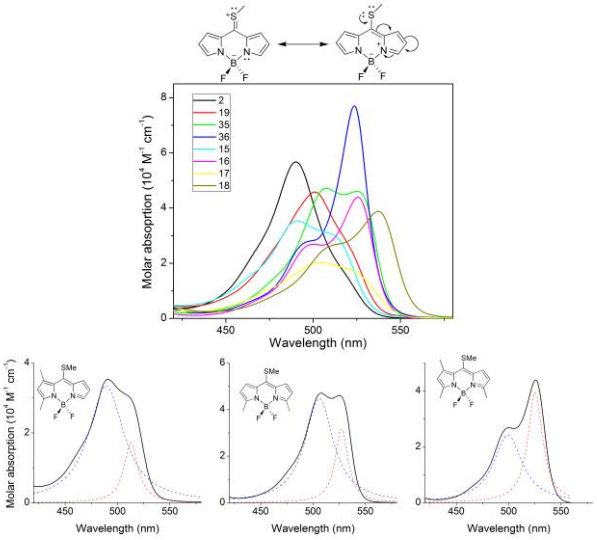

Figure 3. Main resonance structures resulting from the electronic coupling of the 8-methylthio group with the BODIPY core and absorption spectra of dye **2** and its non-symmetric (**15**-**19**) and symmetric (**35**-**36**) alkylated derivatives. For the sake of clarity, the absorption band of selected representative compounds (**15**, **35** and **16**) has been deconvoluted in two lorentzians.

The presence of such new delocalization induced by the 8-methylthio is checked by comparison with its tetramethylated counterpart 36[9] (Table 7). The steric hindrance which induces the methyl groups at the adjacent positions 1 and 7 avoids a coplanar disposition of the methylthio group with the chromophore and the subsequent electronic coupling. As consequence, the spectral bands shapes fully resemble to those of BODIPYs. In return, the fluorescence signal is almost completely quenched, likely owing to the population of a twisted intramocular charge transfer (TICT)[22] state (Table 7). Indeed, even in the reference non-methylated compound 2 the fluorescence efficiency decreases with the solvent polarity (from 75% in cylohexane to 34% in methanol)[9] suggesting the tendency of the electron donor 8-methylthio fragment to activate ICT phenomena.

Table 7. Photophysical properties of the non-symmetric 8-methylthio-BODIPYs in diluted solutions of tetrahydrofuran (2μM). The reported data for the reference compound **2** and related symmetric derivatives **35** and **36** are also included for comparison.[9]

Cmpd	Structure	λ_{ab} (nm)	$\varepsilon_{max}\cdot10^{-4}$ (M^{-1} cm^{-1})	λ_{fl} (nm)	ϕ	τ (ns)	k_{fl} (10^8 s^{-1})	k_{nr} (10^8 s^{-1})
2	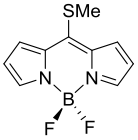	490.0	5.7	532.0	0.41	4.21	0.98	1.39
19	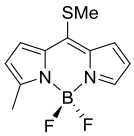	500.5	4.7	532.0	0.59	4.68	1.26	0.86
35		508.0 525.0	4.8 4.6	538.0	0.78	6.53	1.23	0.34
15		490.5	3.6	530.0	0.10	0.20(84%) 4.30(16%)	-	-
16		525.5	4.5	536.0	0.34	2.47(92%) 5.38(8%)	-	-
36		523.0	7.5	536.0	0.006	-	-	-
17	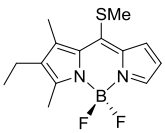	511.0	2.1	533.0	0.036	0.30(98%) 2.64(2%)	-	-
18	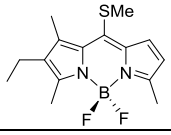	537.5	4.1	554.0	0.39	0.91(8%) 3.04(92%)	1.27	2.02

In view of these preliminary results, in the following lines we will analyze in depth the effect of the alkylation on the electron coupling ability of the 8-methylthio group with the dipyrrin core and the ICT promotion probability (see compounds in Table 2).

Methylation at position 3 (compound **19**) increases the absorbance at lower energies, which becomes almost equal to the absorbance at higher energies upon additional methylation at the opposite position 5 (compound **35** in Figure 3). Beyond this point further alkylation (**16** and **18**) provides an absorption band with the highest absorption probability at lower energies, matching the spectra usually recorded for BODIPYs. On the other hand, the absorption spectra of compound bearing just one alkylated pyrrole (**15** and **17**) reminds of that recorded for compound **19**, with a clear contribution of the new shoulder at higher energies (Figure 3). It is noteworthy that while the shape of the absorption band changes with alkylation, the shape of fluorescence band keeps unaltered (Figure 4). The steric hindrance provided by the methylation at the adjacent position 1 could hamper the resonance interaction of the 8-methylthio fragment in compounds **15**-**18**. Nevertheless, and in line with the results detailed in the preceding section (8-phenyl-BODIPYs), such constriction should not be high enough as to avoid the coplanar disposition, considering the smaller size of the methylthio fragment. These spectral features suggest that there is a subtle balance between both extreme mesomeric forms (Figure 3) in the ground state, which can be tuned by methylation of the chromophore. Thus, the contribution from the cyanine-like delocalized framework (long-wavelength part) is enhanced by alkylation of both pyrroles (mainly at α–positions), whereas the new resonant form (short-wavelength part) by selective alkylation of one pyrrole. In other words, the symmetric alkylation of the dipyrrin core implies that the BODIPY is less acceptor, thereby the resonance interaction from the donor methylthio group is less favored. Indeed, the localized negative

charge onto the 8-sulphur atom progressively increases with the alkylation degree (from -0.15 for compound **2** to around -0.26 for **16** and **18**, see Figure S5) suggesting that the electron lone pair of the sulphur tends to be more localized in this atom rather than delocalized in the indacene core upon alkylation. The only exception is the compound **36** (charge down to -0.18, Figure S5), which undergoes TICT from the electronically decoupled donor 8-methylthio fragment by steric reasons.

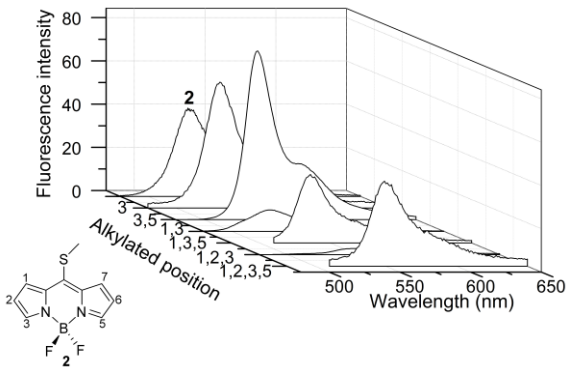

Figure 4. Evolution of the fluorescence spectra with regard to the alkylated chromophoric position of the BODIPYs bearing the 8-methylthio group (compound **2**).

Another striking characteristic of the 8-methylthioBODIPYs is the marked sensibility of the fluorescence response (efficiency and lifetime) with alkylation (Figure 4 and Table 7). The α-methylation (compound **19** and mainly **35**) enhances the fluorescence quantum yield (from 41% in 2 to 78% in 35, Table 7) and enlarges the lifetime (from 4.2 ns to 6.3 ns, respectively, Figure 5). This can be understood considering the aforementioned less acceptor character of the BODIPY upon alkylation, which should reduce the ICT population. Indeed, dye **35** shows similar values regardless of the media (95% and 84% in cyclohexane and methanol respectively).[9] However, in derivatives with just one pyrrole alkylated (**15** and **17**) the fluorescence quantum yield drops drastically (down to 10% and 3%, respectively) and the fluorescence decay curves becomes biexponential, with a fast main lifetime (down to 200-300 ps, Figure 5). The fluorescence response is recovered upon methylation at the opposite pyrrole (**16** and **18**, respectively). Thus, the lifetimes become longer (but still a second exponential is required, see **17** *vs* **18** in Figure 5) and the fluorescence quantum yield increases up to 39% (Table 7).

Therefore, the selective alkylation of one chromophoric pyrrole exerts a deep impact in the fluorescent performance of these compounds. In the preceding sections it was highlighted that such non-symmetric substitution pattern could enhance the non-radiative deactivation owing to the generated charge separation between the pyrroles. Such electronic effect seems to be a key issue in the BODIPYs bearing the 8-methylthio fragment, likely owing to its claimed selective electron coupling with one chromophoric pyrrole. Thus, alkylation of just one pyrrole strengthens the charge separation between the pyrroles and enhances the ICT process induced by the 8-methylthio moiety leading to an effective quenching of the fluorescence emission (see for example compounds **15** and **17**).

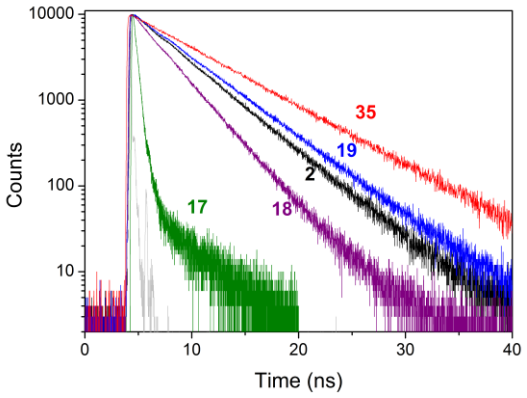

Figure 5. Fluorescence decay curves of selected BODIPYs (**2**, **17**-**19** and **35**) bearing the 8-methylthio group but with the dipyrrin core alkylated at different positions.

Conclusions

We have prepared 5 new non-symmetric Biellmann BODIPY (NSBB) dyes with different alkyl substitutions on each pyrrole rings. These NSBBs displayed excellent reactivity in both the Liebeskind-Srogl cross-coupling and the desulfitative reduction reactions in short reaction times and mild conditions. As a result, BODIPYs with different functionality at the key meso position have been developed with a controlled and selective alkylation pattern. The combined analysis of these novel non-symmetric BODIPYs with the related symmetric ones (commercially available or reported in the bibliography), provides meaningful insights into the molecular structure effect onto the photophysical signatures of these dyes. In this regard, the alkylation promotes modest spectral shifts, albeit opposite depending on the linkage position (bathochromic in positions 3 and 5, or 2 and 6 but hypsochromic at 1 and 7, or 8), and in all cases excellent fluorescence efficiencies (approaching 90%). In contrast, the free rotational motion of the 8-phenyl group drastically reduces the emission signal. Strong steric hindrance (i.e., methylation at both adjacent positions, not partial) are required to block the ring in a nearly ortogonal disposition and completely avoid its deleterious impact into the fluorescence response. Finally, the 8-methylthio fragment induces remarkable changes both in the spectral bands and in the fluorescence efficiency, depending of the alkylation degree and position at the dipyrrin framework. On one hand, noticeable hypsochromic shifts are recorded in the absorption spectra owing to the electronic coupling, which tend to be less feasible upon alkylation. On the other hand, bright fluorescence emissions can be achieved mainly upon symmetric methylation of the BODIPY to avoid ICT processes, which efficiently quenches the fluorescence if the 8-methylthio group is forced to adopt a perpendicular disposition or upon selective alkylation of just one

pyrrole. We believe that the reached guidelines in this work will serve as orientation for the researchers interested in organic fluorophores to design novel BODIPYs for specific applications. With all this insight in hand, it should be possible to judiciously design axially chiral non-symmetric BODIPYs and BODIPY dimers and oligomers with specific properties. Our groups are working on these new avenues and the results will be reported in due course.

Experimental Section

General Information

Synthesis and characterization. Starting materials and reagents used in the preparation of BODIPYs are commercially available unless otherwise noted. The solvents were distilled and dried according to standard procedures before use. Unless stated otherwise, all reactions were performed in oven- and or flame-dried glassware. Reaction progress was monitored by TLC (Merck silica gel plates with F-254 indicator) and the spots were visualized under UV light (254 or 365 nm). Flash column chromatography was performed using silica gel Kieselgel 60 (70-230 mesh) and mixture of ethyl acetate and hexanes as the eluent. Spectral data of the known compounds were in accordance with the literature data. ^{1}H and ^{13}C NMR spectra were acquired on a Bruker Advance III spectrometers (500 or 400 MHz for ^{1}H and 125 or 101 MHz for ^{13}C) in deuteriochloroform ($CDCl_3$) with either tetramethylsilane (TMS) (0.00 ppm ^{1}H, 0.00 ppm ^{13}C) or chloroform (7.26 ppm ^{1}H, 77.16 ppm ^{13}C) or as internal reference unless otherwise stated.[23] Data are reported in the following order: chemical shift in ppm, multiplicities (br (broadened), s (singlet), d (doublet), t (triplet), q (quartet), sex (sextet), hep (heptet), m (multiplet), exch (exchangeable), app (apparent)), coupling constants *J* (Hz), and integration. Infrared spectra were recorded on a Perkin Elmer Spectrum 100 FTIR spectrophotometer. Peaks are reported (cm^{-1}) with the following relative intensities: s (strong, 67-100%), m (medium 40-66%), and w (weak 20-39%). Melting points were determined on a Stanford Research Systems EZ-Melt apparatus and were uncorrected. HRMS samples were ionized by ESI+ and recorded via the TOF method. Copper(I) thiophene-2-carboxylate (CuTC),[24] were prepared according to the literature procedures.

Synthesis and characterization of compounds

General procedure for the synthesis of thioketones 8-12 (GP1). In a two-necked flask, one connected to a trap of NaOH, was added THF (0.16 M) and the corresponding mixture of pyrroles 4-7 (1: 2 equiv.). The reaction mixture was immersed in an ice bath and thiophosgene (1.5 eqiv.) was added dropwise with vigorous stirring at 0 °C. After 15 min was added MeOH (15 mL) and the mixture stirred for 30 min at room temperature. The solvents were removed in vacuo and the residue was left under vacuum for 2 hours. The crude product was adsorbed on silica gel and it was purified by column chromatography (1.0-5.0% ethyl acetate / hexanes).

General Procedure for the synthesis of Non-symmetric Biellmann BODIPYs 15-19 (GP2). To a solution of the corresponding thioketone 8-12 (1 equiv.) in anhydrous dichloromethane (0.2 M) was added methyl iodide (5 equiv.) dropwise at room temperature. The reaction mixture was stirred for 12 h it to completion (monitored by TLC). The solvent was removed under reduced pressure to give a gummy solid which was left under vacuum for one hour. The residue was dissolved in anhydrous dichloromethane (0.2 M) under nitrogen atmosphere, was added triethylamine (1.4 equiv.) dropwise at room temperature. After stirring for 30 min was added $BF_3{\cdot}OEt_2$ (1.4 equiv.). The mixture was stirred for 5 min and monitored by TLC product formation was observed. The solvent was removed in vacuum. The reaction crude was dissolved in AcOEt and adsorbed onto silica gel. The compound was purified by column chromatography (1.0-3.0% ethyl acetate / hexanes).

General Procedure for the Liebeskind-Srogl cross-coupling reaction (GP3). An oven-dry Schlenk tube, equipped with a stir bar, was charged with the corresponding non-symmetric Biellmann BODIPY **15**-**19** (1 eq), phenyl boronic acid (3 equiv.) and dry THF (0.03 M) under N_2. The stirred solution was sparged with N_2 for 10 min., whereupon CuTC (3 equiv.), $Pd_2(dba)_3$ (2.5 mol%) and TFP (7.5 mol%) were added under N_2. The reaction mixture was immersed into a pre-heated oil bath at 55 °C. After TLC showed that the reaction went to completion, the reaction mixture was allowed to reach rt and was adsorbed on SiO_2-gel. After flash-chromatography (SiO_2-gel, EtOAc/hexanes gradient) purification, mesophenyl BODIPY´s were obtained as highly-colored crystalline solids.

General Procedure for the Desulfitative reduction reaction (GP4). An oven-dry Schlenk tube, equipped with a stir bar, was charged with the corresponding non-symmetric Biellmann BODIPY **15**-**19** (1 eq), triethylsilane (3 equiv.) and dry THF (0.06 M) under N_2. The stirred solution was sparged with N_2 for 10 min., whereupon CuTC (3 equiv.), $Pd_2(dba)_3$ (2.5 mol%) and TFP (7.5 mol%) were added under N_2. The reaction mixture was immersed into a pre-heated oil bath at 55 °C. After TLC showed that the reaction went to completion, the reaction mixture was allowed to reach rt and was adsorbed on SiO_2-gel. After flash-chromatography (SiO_2-gel, EtOAc/hexanes gradient) purification, bodipy's were obtained as highly-colored crystalline solids.

Compound 8: According to GP1. Pyrrole **5** (0.1000 g, 1.4916 mmol, 1.0 equiv.), 2,4-dimethylpyrrole **4** (0.2388 g, 2.9833 mmol, 2.0 equiv.), and thiophosgene (0.2573 g, 2.2375 mmol, 1.5 equiv.). The desired product was obtained as a purple crystals (0.1314 g, 43 % yield); mp 90-91 °C; TLC (15% EtOAc/hexanes, R_f = 0.20); IR (KBr, cm-1): 3382 (m), 3336 (m), 3089 (w), 2911 (w), 1721 (w), 1560 (w), 1535 (w), 1484 (m), 1474 (m), 1433 (s), 1408 (s), 1394 (m), 1392 (s), 1337 (m), 1301 (m), 1258 (m), 1145 (w), 1127 (w), 1115 (w), 1092 (m), 1040 (m), 1023 (w), 1003 (m), 944 (m), 880 (w), 843 (w), 791 (m), 747 (s), 714 (m), 646 (m), 579 (m); ^{1}H NMR (400 MHz, $CDCl_3$): δ= 9.68 (br, 1H), 9.12 (br, 1H), 7.10 (s, 1H), 6.69 (s, 1H), 6.32 (s, 1H), 5.98 (s, 1H), 2.25 (s, 6H); ^{13}C NMR (101 MHz, $CDCl_3$): δ= 192.6, 138.2, 137.7, 136.6, 128.7, 126.8, 115.8, 115.2, 111.6, 15.3, 13.4; HRMS (ESI+): *m/z* calcd. for $C_{11}H_{13}N_2S$ $[M+H]^+$, 205.0794, found 205.0796.

Compound 9: According to GP1. 2-methylpyrrole **7** (0.0426g, 0.5 mmol, 1.0 equiv.), 2,4-dimethylpyrrole **4** (0.1000 g, 1.0 mmol, 2.0 equiv.), and thiophosgene (0.0906 g, 0.8 mmol, 1.5 equiv.). The desired product was obtained as a purple solid (0.0515 g, 45 % yield); mp 99-101 °C; TLC (15% EtOAc/hexanes, R_f = 0.35); IR (KBr, cm-1): 3293 (m), 2911 (w), 1555 (m), 1490 (s), 1427 (s), 1367 (s), 1336 (m), 1254 (s), 1202 (s), 1142 (m), 1036 (s), 979 (m), 944 (m), 841 (w), 782 (m), 716 (m), 644 (m); ^{1}H NMR (400 MHz, $CDCl_3$): δ= 9.46 (br, 1H), 9.01 (br, 1H), 6.56 (s, 1H), 5.99 (s, 1H), 5.87 (s, 1H), 2.23 (s, 3H), 2.17 (s, 6H); ^{13}C NMR (101 MHz, $CDCl_3$): δ= 190.5, 139.6, 137.8, 136.8, 135.8, 127.2, 118.0, 114.7, 111.3, 15.1, 13.6, 13.3; HRMS (ESI+): *m/z* calcd. for $C_{12}H_{15}N_2S$ $[M+H]^+$, 219.0950; found 219.0955.

Compound 10: According to GP1. Pyrrole **5** (0.248 g, 3.7 mmol, 1.0 equiv.), 3-ethyl-2,4-dimethylpyrrole **6** (0.913 g, 7.4 mmol, 2.0 equiv.), and thiophosgene (0.6391 g, 5.5 mmol, 1.5 equiv.). The desired product was obtained as a purple solid (0.3859 g, 45 % yield); mp 89-91 °C; TLC

(15% EtOAc/hexanes, R_f = 0.40); IR (KBr, cm-1): 3436 (m), 3395 (m), 3348 (m), 2924 (m), 2854 (m), 1731 (w), 1526 (s), 1397 (s), 1285 (m), 1234 (m), 1095 (s), 1060 (s), 1028 (s), 987 (m), 908 (m), 881 (m), 798 (w), 746 (s), 705 (m), 640 (m), 590 (m); ^{1}H NMR (400 MHz, $CDCl_3$): δ= 9.69 (br, 1H), 9.08, (br, 1H), 7.12 (s, 1H), 6.68 (s, 1H), 6.33(s, 1H), 2.41 (c, J = 8.0 Hz, 2H), 2.23 (s, 6H), 1.08 (t, J = 8.0 Hz, 3H); ^{13}C NMR (101 MHz, $CDCl_3$): δ= 191.4, 138.2, 136.2, 135.8, 128.0, 126.9, 126.5, 115.7, 111.5, 17.6, 15.0, 13.3, 11.9; HRMS (ESI+): *m/z* calcd. for $C_{13}H_{17}N_2S$ $[M+H]^+$, 233.1107; found 233.1116.

Compound 11: According to GP1. 2-methylpyrrole **7** (0.3006 g, 3.7 mmol, 1.0 equiv.), 3-ethyl-2,4-dimethylpyrrole **6** (0.913 g, 7.4 mmol, 2.0 equiv.), and thiophosgene (0.6391 g, 5.5 mmol, 1.5 equiv.). The desired product was obtained as a red solid (0.2000 g, 22 % yield); mp 118-120 °C; TLC (15% EtOAc/hexanes, R_f = 0.35); IR (KBr, cm-1): 3294 (s), 2962 (m), 2924 (m), 2856 (m), 1724 (w), 1552 (w), 1478 (s), 1445 (s), 1412 (s), 1370 (s), 1336 (s), 1244 (s), 1108 (s), 1044 (s), 939 (s), 905 (m), 791 (m), 720 (w), 624 (w); ^{1}H NMR (400 MHz, $CDCl_3$): δ= 9.46 (br, 1H). 8.99 (br, 1H), 6.63 (m, 1H), 6.08 (m, 1H), 2.41 (c, J = 8.0 Hz, 2H), 2.34 (s, 3H), 2.24 (s, 3H), 2.23 (s, 3H), 1.08 (t, J = 8.0 Hz, 3H); ^{13}C NMR (101 MHz, $CDCl_3$): δ= 189.77, 139.2, 137.8, 135.5, 134.7, 127.5, 125.5, 117.9, 111.3, 17.6, 15.1, 13.8, 13.2, 11.9; HRMS (ESI+): *m/z* calcd. for $C_{14}H_{19}N_2S$ $[M+H]^+$, 247.1263; found 247.1265.

Compound 12: According to GP1. Pyrrole **5** (0.1000 g, 1.4 mmol, 1.0 equiv.), 2-methylpyrrole **7** (0.2420 g, 3.0 mmol, 2.0 equiv.), and thiophosgene (0.257 g, 2.2 mmol, 1.5 equiv.). The desired product was obtained as a red solid (0.2000 g, an inseparable mixture of 12 and 13 was obtained); mp of the mixture (12 and 13) 68-70 °C; TLC (15% EtOAc/hexanes, R_f = 0.40); IR (KBr, cm-1): 3287 (m), 1554 (w), 1527 (m), 1485 (m), 1458 (m), 1396 (s), 1377 (s), 1335 (m), 1291 (m), 1259 (m), 1230 (m), 1195 (m), 1097 (s), 1073 (m), 1025 (s), 1004 (m), 986 (m), 908 (m), 878 (m), 797, (m), 748 (m), 651 (m), 590 (w); $_1$H NMR (400 MHz, $CDCl_3$): δ= 9.86 (br, 1H), 9.71 (br, 1H), 7.04 (s, 1H), 6.93 (m, 2H), 6.31 (m, 1H), 6.07 (m, 1H), 2.21 (s, 3H); ^{13}C NMR (101 MHz, $CDCl_3$): δ= 189.9, 140.6, 137.9, 137.5, 126.9, 116.8, 114.1, 112.1, 112.0 13.4; HRMS (ESI+): *m/z* calcd. for $C_{10}H_{11}N_2$ $[M+H]^+$, 191.0637; found 191.0637.

Compound 15: According to GP2. Thioketone **8** (0.067 g, 0.3 mmol, 1.0 equiv.), iodomethane (0.2321 g, 1.5 mmol, 5.0 equiv.), triethylamine (0.0427 g, 0.4 mmol, 1.4 equiv.), and boron trifluoride diethyl etherate (0.0649 g, 0.4 mmol, 1.4 equiv.). The desired product was obtained as an orange crystals (0.0547 g, 63% yield); mp 102-104 °C; TLC (15% EtOAc/hexanes, R_f = 0.30); IR (KBr, cm-1): 3416 (w), 2967 (w), 2917 (w), 1727 (w), 1534 (m), 1516 (s), 1499 (m), 1470 (m), 1456 (m), 1435 (m), 1405 (s), 1369 (s), 1329 (m), 1315 (m), 1289 (m), 1235 (m), 1193 (s), 1156 (s), 1100 (s), 1058 (s), 1003 (s), 957 (s), 804 (m), 742 (m), 710 (w), 608 (w); ^{1}H NMR (400 MHz, $CDCl_3$): δ= 7.49 (s, 1H), 7.15 (s, 1H), 6.36 (s, 1H), 6.09 (s, 1H), 2.64 (s, 3H), 2.48 (s, 3H), 2.46 (s, 3H); ^{13}C NMR (101 MHz, $CDCl_3$): δ= 160.2, 147.0, 146.5, 136.8, 135.1, 133.5, 125.7, 123.5, 115.8, 22.0, 17.7, 14.0; HRMS (ESI+): *m/z* calcd. for $C_{12}H_{14}BF_2N_2S$ $[M+H]^+$, 267.0936; found 267.0933.

Compound 16: According to GP2. Thioketone **9** (0.1500 g, 0.7 mmol, 1.0 equiv.), iodomethane (0.4877 g, 3.4 mmol, 5.0 equiv.), triethylamine (0.0980 g, 1.0 mmol, 1.4 equiv.), and boron trifluoride diethyl etherate (0.1365 g, 1.0 mmol, 1.4 equiv.). The desired product was obtained as a yellow crystals (0.0934 g, 49% yield); mp 123-125 °C; TLC (15% EtOAc/hexanes, R_f = 0.50); IR (KBr, cm-1): 3417 (w), 2966 (w), 2926 (w), 1727 (w), 1543 (s), 1488 (m), 1455 (m), 1370 (w), 1289 (s), 1215 (m), 1179 (s), 1151 (s), 1109 (m), 1073 (s), 1029 (m), 975 (s), 792 (w), 775 (w), 736 (w); ^{1}H NMR (400 MHz, $CDCl_3$): δ= 7.25 (d, J = 4.0 Hz, 1H), 6.23 (d, J = 4.0 Hz, 1H), 6.11 (s, 1H), 2.60 (s, 3H), 2.56 (s, 9H); ^{13}C NMR (101 MHz, $CDCl_3$): δ= 157.9, 154.5, 144.5, 143.1, 135.8, 134.3, 128.1, 122.7, 118.2, 22.6, 17.0, 14.9, 14.8; HRMS (ESI+): *m/z* calcd. for $C_{13}H_{16}BF_2N_2S$ $[M+H]^+$, 281.1092; found 281.1088.

Compound 17: According to GP2. Thioketone **10** (0.1400 g, 0.6 mmol, 1.0 equiv.), iodomethane (0.4276g, 3.0 mmol, 5.0 equiv.), triethylamine (0.0856 g, 0.84 mmol, 1.4 equiv.), and boron trifluoride diethyl etherate (0.1197 g, 0.8 mmol, 1.4 equiv.). The desired product was obtained as a yellow crystals (0.0517 g, 29% yield); mp 109-111 °C; TLC (15% EtOAc/hexanes, R_f = 0.40); IR (KBr, cm-1): 3417 (w), 3106 (w), 2964 (w), 2917 (w), 2864 (w), 1725 (w), 1539 (s), 1459 (m), 1406 (m), 1389 (m), 1362 (m), 1341 (m), 1282 (m), 1260 (w), 1220 (m), 1192 (m), 1168 (s), 1141 (m), 1121 (m), 1089 (m), 1071 (s), 1032 (m), 1000 (m), 954 (m), 756 (w), 735 (w), 546 (w); ^{1}H NMR (400 MHz, $CDCl_3$): δ= 7.52 (s, 1H), 7.19 (m, 1H), 6.40 (m, 1H), 2.68 (s, 3H), 2.56 (s, 3H), 2.51 (s, 3H), 2.41 (c, J = 8.0 Hz, 2H), 1.05 (t, J = 8.0 Hz, 3H); ^{13}C NMR (101 MHz, $CDCl_3$): δ= 161.5, 144.4, 142.2, 136.2 136.1, 135.8, 133.8, 124.9, 115.3, 22.3, 17.3, 14.7, 14.4, 13.3; HRMS (ESI+): *m/z* calcd. for $C_{14}H_{18}BF_2N_2S$ $[M+H]^+$, 295.1249; found 295.1251.

Compound 18: According to GP2. Thioketone **11** (0.0490 g, 0.2 mmol, 1.0 equiv.), iodomethane (0.1457 g, 1.0 mmol, 5.0 equiv.), triethylamine (0.0285 g, 0.28 mmol, 1.4 equiv.), and boron trifluoride diethyl etherate (0.0395 g, 0.3 mmol, 1.4 equiv.). The desired product was obtained as a red crystals (0.0193 g, 32% yield); mp 62-64 °C; TLC (15% EtOAc/hexanes, R_f = 0.60); IR (KBr, cm-1): 3434 (w), 2959 (w), 2923 (w), 1742 (w), 1529 (m), 1499 (m), 1474 (s), 1411 (m), 1398 (m), 1383 (m), 1371 (m), 1289 (s), 1260 (m), 1233 (m), 1195 (s), 1170 (s), 1100 (m), 1051 (m), 991 (m), 972 (m), 942 (m), 832 (w), 769.3 (m), 748 (m), 540 (w); ^{1}H NMR (400 MHz, $CDCl_3$): δ= 7.23 (d, J = 4.0 Hz, 1H), 6.19 (d, J = 4.0 Hz, 1H), 2.58 (s, 3H), 2.55 (m, 9H), 2.41 (c, J = 8.0 Hz, 2H), 1.06 (t, J = 8.0 Hz, 3H); ^{13}C NMR (101 MHz, $CDCl_3$): δ= 158.6, 153.2, 141.3, 140.5, 135.7, 135.2, 134.6, 127.2, 117.3, 22.7, 17.3, 14.8, 14.6, 14.0, 13.1; HRMS (ESI+): *m/z* calcd. for $C_{15}H_{20}BF_2N_2S$ $[M+H]^+$, 309.1406; found 309.1407.

Compound 19: According to GP2. Mixture of **12** and **13** (0.1600 g, 0.8 mmol, 1.0 equiv.), iodomethane (0.6444 g, 4.0 mmol, 5.0 equiv.), triethylamine (0.1141 g, 1.1 mmol, 1.4 equiv.), and boron trifluoride diethyl etherate (0.1804 g, 1.1 mmol, 1.4 equiv.). The desired product was obtained as a yellow crystals (0.0849 g, 40% yield); mp 85-87 °C; TLC (15% EtOAc/hexanes, R_f = 0.25); IR (KBr, cm-1): 3424 (w), 3106 (w), 1722 (w), 1528 (m), 1494 (m), 1472 (w), 1454 (w), 1411 (m), 1376 (m), 1335 (w), 1259 (s), 1182 (m), 1138 (s), 1103 (s), 1073 (s), 1040 (m), 1025 (m), 1000 (m), 938 (w), 884 (w), 768 (w), 751 (w); ^{1}H NMR (400 MHz, $CDCl_3$): δ= 7.66 (s, 1H), 7.42 (m, 1H), 7.29 (m, 1H), 6.47 (s, 1H), 6.34 (m, 1H), 2.80 (s, 3H), 2.62 (s, 3H); ^{13}C NMR (101 MHz, $CDCl_3$): δ= 159.7, 148.5, 139.1, 135.9, 133.5, 130.1, 125.9, 120.6, 116.8, 21.1, 15.2; HRMS (ESI+): *m/z* calcd. for $C_{11}H_{12}BF_2N_2S$ $[M+H]^+$, 253.0779; found 253.0774.

Compound 20: According to GP3. **15** (0.0100 g, 0.04 mmol 1.0 equiv.), phenylboronic acid (0.0137 g, 0.11 mmol, 3.0 equiv), CuTC (0.0215 g, 0.11 mmol, 3.0 equiv.), $Pd_2(dba)_3$ (0.001 g, 0.001 mmol, 2.5 mol%), and tri-2-furylphosphine (0.001 g, 0.003 mmol, 7.5 mol%). Time of reaction 1.25 h. The desired product was obtained as an orange crystals (0.056 g, 50 % yield); mp 135-137 °C; TLC (15% EtOAc/hexanes, R_f = 0.45); IR (KBr, cm-1): 3440 (w), 1579 (s), 1552 (s), 1521 (m), 1459 (w), 1392 (s), 1341 (w), 1288 (m), 1221 (w), 1172 (m), 1141 (s), 1094 (m), 1076 (m), 1044 (m), 1002 (m), 982 (m), 941 (w), 771 (w), 727 (m); ^{1}H NMR (400 MHz, $CDCl_3$): δ= 7.68 (s, 1H), 7.49 (m, 3H), 7.35 (m, 2H), 6.40 (s, 1H), 6.37 (s, 1H), 6.13 (s, 1H), 2.63 (s, 3H), 1.53 (s, 3H); ^{13}C NMR (101 MHz, $CDCl_3$): δ= 162.2, 147.2, 143.5, 138.8, 134.9, 134.1, 133.7, 129.5, 128.9, 128.6, 127.2, 123.4, 116.2, 15.3, 15.1; HRMS (ESI+): *m/z* calcd. for $C_{17}H_{16}BF_2N_2$ $[M+H]^+$, 297.1372; found 297.1370.

Compound 21: According to GP3. **16** (0.0400 g, 0.14 mmol 1.0 equiv.), phenylboronic acid (0.0522 g, 0.42 mmol, 3.0 equiv), CuTC (0.0817 g, 0.42 mmol, 3.0 equiv.), $Pd_2(dba)_3$ (0.0032 g, 0.0035 mmol, 2.5 mol%), and tri-2-furylphosphine (0.0024 g, 0.0105 mmol, 7.5 mol%). Time of reaction 1.50 h. The desired product was obtained as a red crystals (0.0258 g, 58 % yield); mp 143-144 °C; TLC (15% EtOAc/hexanes, R_f = 0.55); IR (KBr, cm-1): 3420 (w), 2927 (w), 1578 (w), 1545 (s), 1520 (m), 1490 (m), 1467 (m), 1443 (w), 1411 (w), 1373 (w), 1292 (s), 1217 (w), 1181 (m), 1149 (s), 1103 (w), 1086 (w), 1069 (w), 1026 (w), 989 (m) 811 (w), 777 (w), 735 (m); ^{1}H NMR (400 MHz, $CDCl_3$): δ= 7.39 (m, 3H), 7.25 (m, 2H), 6.28 (s, 1H), 6.08 (s, 1H), 5.98 (s, 1H), 2.53 (s, 6H), 1.41 (s, 3H); ^{13}C NMR (101 MHz, $CDCl_3$): δ= 158.6, 155.3, 144.5, 142.0, 135.3, 134.4, 132.3, 129.2, 129.0, 129.0, 128.4, 122.1, 118.1, 15.0, 14.8; HRMS (ESI+): *m/z* calcd. for $C_{18}H_{18}BF_2N_2$ $[M+H]^+$, 311.1529; found 311.1535.

Compound 22: According to GP3. **17** (0.0100 g, 0.03 mmol 1.0 equiv.), phenylboronic acid (0.0124 g, 0.10 mmol, 3.0 equiv), CuTC (0.0194 g, 0.10 mmol, 3.0 equiv.), $Pd_2(dba)_3$ (0.0007 g, 0.8 mmol, 2.5 mol%), and tri-2-furylphosphine (0.0006 g, 0.0023 mmol, 7.5 mol%). Time of reaction 1.00 h. The desired product was obtained as an orange crystals (0.0078 g, 71 % yield); mp 114-116 °C; TLC (15% EtOAc/hexanes, R_f = 0.55); IR (KBr, cm-1): 3431 (w), 2927 (w), 1730 (w), 1578 (w), 1544 (s), 1520 (m), 1490 (m), 1465 (m), 1442 (w), 1372 (w), 1292 (m), 1217 (w), 1182 (m), 1153 (s), 1104 (m), 1068 (m), 1029 (w), 989 (m), 812 (w), 779 (w), 735 (m); ^{1}H NMR (400 MHz, $CDCl_3$): δ= 7.62 (s, 1H), 7.49 (m, 3H), 7.35 (m, 2H), 6.33 (s, 2H), 2.62 (s, 3H), 2.35 (c, J = 8.0 Hz, 2H), 1.45 (s, 3H), 1.02 (t, J = 8.0 Hz, 3H); ^{13}C NMR (101 MHz, $CDCl_3$): δ= 162.5, 142.3, 142.1, 137.4, 136.0, 134.7, 134.5, 133.5, 129.3, 128.9, 128.5, 126.0, 115.5, 17.3, 14.4, 13.4, 12.5; HRMS (ESI+): *m/z* calcd. for $C_{19}H_{20}BF_2N_2$ $[M+H]^+$, 325.1686; found 325.1684.

Compound 23: According to GP3. **18** (0.0115 g, 0.03 mmol 1.0 equiv.), phenylboronic acid (0.0136 g, 0.10 mmol, 3.0 equiv), CuTC (0.0226 g, 0.10 mmol, 3.0 equiv.), $Pd_2(dba)_3$ (0.0007 g, 0.001 mmol, 2.5 mol%), and tri-2-furylphosphine (0.0005 g, 0.0023 mmol, 7.5 mol%). Time of reaction 1.25 h. The desired product was obtained as an orange crystals (0.0072 g, 60 % yield); mp 123-124 °C; TLC (15% EtOAc/hexanes, R_f = 0.60); IR (KBr, cm-1): 3441 (w), 2962 (w), 2927 (w), 2869 (w), 1575 (w), 1545 (s), 1492 (m), 1474 (m), 1402 (w), 1368 (w), 1294 (m), 1264 (m), 1222 (m), 1174 (s), 1153 (s), 1108 (m), 1068 (m), 1027 (m), 992 (m), 971 (m), 734 (w); ^{1}H NMR (400 MHz, $CDCl_3$): δ= 7.46 (m, 3H), 7.32 (m, 2H), 6.28 (m, 1H), 6.11 (m, 1H), 2.59 (s, 6H), 2.34 (c, J = 8.0 Hz, 2H), 1.41 (s, 3H), 1.01 (t, J = 8.0 Hz, 3H); ^{13}C NMR (101 MHz, $CDCl_3$): δ= 158.8, 153.6, 140.9, 140.4, 135.1, 134.8, 134.7 134.7, 132.1, 129.1, 128.4, 127.9, 117.2, 17.3, 14.7, 14.6, 13.1, 12.3; HRMS (ESI+): *m/z* calcd. for $C_{20}H_{22}BF_2N_2$ $[M+H]^+$, 339.1842; found 339.1850.

Compound 24: According to GP3. **19** (0.0400 g, 0.16 mmol 1.0 equiv.), phenylboronic acid (0.0582 g, 0.48 mmol, 3.0 equiv), CuTC (0.0908 g, 0.48 mmol, 3.0 equiv.), $Pd_2(dba)_3$ (0.0036 g, 0.0040 mmol, 2.5 mol%), and tri-2-furylphosphine (0.0028 g, 0.0120 mmol, 7.5 mol%). Time of reaction 1.50 h. The desired product was obtained as an orange crystals (0.0362 g, 81 % yield); mp 97-98 °C; TLC (15% EtOAc/hexanes, R_f = 0.40); IR (KBr, cm-1): 3435 (w), 3144 (w), 2917 (w), 1582 (s), 1562 (s), 1532 (m), 1505 (w), 1469 (w), 1443 (w), 1398 (s), 1354 (m), 1288 (m), 1250 (w), 1221 (w), 1151 (m), 1135 (s), 1106 (m), 1075 (m), 1062 (m), 1023 (m), 982 (m), 939 (w), 883 (w), 806 (w), 749 (w), 719 (m); ^{1}H NMR (400 MHz, $CDCl_3$): δ= 7.78 (s, 1H), 7.50 (m, 5H), 6.87 (m, 1H), 6.76 (m, 1H), 6.46 (s, 1H), 6.35 (m, 1H), 2.68 (s, 3H); ^{13}C NMR (101 MHz, $CDCl_3$): δ= 161.4, 144.6, 140.8, 135.8, 134.1, 134.0, 133.1, 130.5, 130.4, 128.9, 128.4, 121.2, 117.2, 15.4; HRMS (ESI+): *m/z* calcd. for $C_{16}H_{14}BF_2N_2$ $[M+H]^+$, 283.1216; found 283.1209.

Compound 25: According to GP4. **15** (0.0150 g, 0.06 mmol 1.0 equiv.), triethylsilane (0.0196 g, 0.17 mmol, 3.0 equiv), CuTC (0.0322 g, 0.17 mmol, 3.0 equiv.), $Pd_2(dba)_3$ (0.0014 g, 0.0015 mmol, 2.5 mol%), and tri-2-furylphosphine (0.0010 g, 0.0045 mmol, 7.5 mol%). Time of reaction 1.25 h. The desired product was obtained as an yellow crystals (0.0109 g, 89 % yield); mp 140-142 °C; TLC (15% EtOAc/hexanes, R_f = 0.25); IR (KBr, cm-1): 3428 (w), 2950 (w), 1610 (s), 1530 (m), 1473 (m), 1460 (m), 1405 (w), 1320 (w), 1260(s), 1181 (m), 1174 (s), 1135 (s), 1056 (m), 968 (m), 780 (w), 756 (w), 685 (w), 643 (w); ^{1}H NMR (400 MHz, $CDCl_3$): δ= 7.63 (s, 1H), 7.18 (s, 1H), 6.91 (m, 1H), 6.42 (s, 1H), 6.14 (s, 1H), 2.58 (s, 3H), 2.25 (s, 3H); ^{13}C NMR (101 MHz, $CDCl_3$): δ= 163.2, 145.0, 139.2, 136.6, 132.7, 126.6, 124.9, 121.4, 116.4, 15.3, 11.5; HRMS (ESI+): *m/z* calcd. for $C_{11}H_{12}BF_2N_2$ $[M+H]^+$, 221.1058; found 221.1056.

Compound 26: According to GP4. **16** (0.0300 g, 0.11 mmol 1.0 equiv.), triethylsilane (0.0374 g, 0.33 mmol, 3.0 equiv), CuTC (0.0613 g, 0.33 mmol, 3.0 equiv.), $Pd_2(dba)_3$ (0.0025 g, 0.0027 mmol, 2.5 mol%), and tri-2-furylphosphine (0.0019 g, 0.0083 mmol, 7.5 mol%). Time of reaction 1.00 h. The desired product was obtained as an orange crystals (0.0232 g, 93 % yield); mp 175-176 °C; TLC (15% EtOAc/hexanes, R_f = 0.30); IR (KBr, cm-1): 3431 (w), 2917 (w), 1609 (s), 1527 (m), 1489 (m), 1462 (m), 1406 (w), 1315 (w), 1248 (s), 1194 (m), 1172 (s), 1138 (s), 1056 (m), 1030 (m), 966 (s), 779 (w), 753 (w), 670 (w), 641 (w); ^{1}H NMR (400 MHz, $CDCl_3$): δ= 7.04 (s, 1H), 6.86 (m, 1H), 6.21 (m, 1H), 6.07 (s, 1H), 2.58(s, 3H), 2.55 (s, 3H), 2.22 (s, 3H); ^{13}C NMR (101 MHz, $CDCl_3$): δ= 159.3, 155.9, 143.2, 134.9, 133.7, 128.5, 123.5, 120.0, 118.4, 15.0, 14.9, 11.4; HRMS (ESI+): *m/z* calcd. for $C_{12}H_{14}BF_2N_2$ $[M+H]^+$, 235.1215; found 235.1211.

Compound 27: According to GP4. **17** (0.0150 g, 0.05 mmol 1.0 equiv.), triethylsilane (0.0178 g, 0.15 mmol, 3.0 equiv), CuTC (0.0292 g, 0.15 mmol, 3.0 equiv.), $Pd_2(dba)_3$ (0.0011 g, 0.0013 mmol, 2.5 mol%), and tri-2-furylphosphine (0.0009 g, 0.0037 mmol, 7.5 mol%). Time of reaction 1.00 h. The desired product was obtained as a red crystals (0.0110 g, 90 % yield); mp 133-135 °C; TLC (15% EtOAc/hexanes, R_f = 0.30); IR (KBr, cm-1): 3430 (w), 2967 (w), 2927 (w), 2864 (w), 1614 (s), 1529 (w), 1450 (w), 1402 (m), 1373 (w), 1285 (m), 1259 (w), 1168 (m), 1146 (m), 1112 (w), 1069 (s), 1033 (s), 1004 (m), 965 (m), 898 (w), 760 (w); ^{1}H NMR (400 MHz, $CDCl_3$): δ= 7.57 (s, 1H), 7.10 (s, 1H), 6.84 (m, 1H), 6.38 (s, 1H), 2.56 (s, 3H), 2.39 (c, J = 8.0 Hz, 2H), 2.16 (s, 3H), 1.07 (t, J = 8.0 Hz, 3H); ^{13}C NMR (101 MHz, $CDCl_3$): δ= 163.4. 141.2, 137.9, 136.3, 134.9, 132.4, 125.3, 123.6, 115.6, 17.3, 14.3, 13.4, 9.5; HRMS (ESI+): *m/z* calcd. for $C_{13}H_{16}BF_2N_2$ $[M+H]^+$, 249.1371; found 249.1368.

Compound 28: According to GP4. **18** (0.0140 g, 0.05 mmol 1.0 equiv.), triethylsilane (0.0158 g, 0.14 mmol, 3.0 equiv), CuTC (0.0259 g, 0.14 mmol, 3.0 equiv.), $Pd_2(dba)_3$ (0.0011 g, 0.0013 mmol, 2.5 mol%), and tri-2-furylphosphine (0.0009 g, 0.0034 mmol, 7.5 mol%). Time of reaction 1.00 h. The desired product was obtained as a red crystals (0.0080 g, 70 % yield); mp 94-95 °C; TLC (15% EtOAc/hexanes, R_f = 0.50); IR (KBr, cm-1): 3436 (w), 2966 (w), 2929 (w), 1612 (s), 1488 (m), 1469 (m), 1457 (m), 1370 (w), 1307 (w), 1254 (m), 1187 (m), 1158 (m), 1105 (m), 1064 (m), 1033 (m), 997 (m), 974 (m) 900 (w), 773 (w); ^{1}H NMR (400 MHz, $CDCl_3$): δ= 6.99 (s, 1H), 6.81 (m, 1H), 6.17 (m, 1H), 2.56 (s, 3H), 2.54, (s, 3H), 2.39 (c, J = 8.0 Hz, 2H), 2.16 (s, 3H), 1.07 (t, J = 8.0 Hz, 3H); ^{13}C NMR (101 MHz, $CDCl_3$): δ= 159.4, 154.3, 139.2, 134.6, 133.6, 133.3, 127.3, 122.5, 117.5, 17.4, 14.8, 14.5, 13.0, 9.5; HRMS (ESI+): *m/z* calcd. for $C_{14}H_{17}BF_2N_2$ $[M+H]^+$, 263.1528; found 263.1532.

Compound 29: According to GP4. **19** (0.0362 g, 0.14 mmol 1.0 equiv.), triethylsilane (0.0501 g, 0.43 mmol, 3.0 equiv), CuTC (0.0821 g, 0.43 mmol, 3.0 equiv.), $Pd_2(dba)_3$ (0.003.2 g, 0.0035 mmol, 2.5 mol%), and tri-2-furylphosphine (0.0024 g, 0.0105 mmol, 7.5 mol%). Time of reaction 1.00 h. The desired product was obtained as a red crystals (0.0266 g,

90 % yield); mp 112-113 °C; TLC (15% EtOAc/hexanes, R_f = 0.26); IR (KBr, cm-1): 3423 (w), 2966 (w), 1609 (s), 1505 (w), 1460 (w), 1404 (m), 1381 (m), 1280 (s), 1176 (m), 1159 (m), 1127 (m), 1077 (m), 1057 (m), 1018 (s), 974 (m), 924 (m), 757 (w), 705 (m); ^{1}H NMR (400 MHz, $CDCl_3$): δ= 7.71 (s, 1H), 7.20 (s, 1H), 7.07 (m, 1H), 6.98 (m, 1H), 6.46 (s, 1H), 6.35 (m, 1H), 2.64 (s, 3H); ^{13}C NMR (101 MHz, $CDCl_3$): δ= 162.4, 141.3, 136.4, 133.7, 133.0, 128.7, 128.3, 121.5, 117.3, 15.4; HRMS (ESI+): *m/z* calcd. for $C_{10}H_{10}BF_2N_2$ $[M+H]^+$, 207.0901; found 207.0899.

Compound 30: An oven-dry flask, equipped with a stir bar, was charged with non-symmetrical Biellmann BODIPY **15** (0.0100 g, 0.04 mmol, 1.0 equiv.), and dry THF (0.02 M). Another flask was charged with NBS (0.0080 g, 0.05 mol, 1.2 eq), and dry THF (0.025 M), this solution is added to the BODIPY dropwise. It was allowed to stir for one hour at room temperature. The crude reaction is neutralized with saturated solution of $NaHCO_3$ (10 mL) and extracted with AcOEt (5 x 5 mL). The organic phase was dried over $MgSO_4$, filtered, and was adsorbed on SiO_2-gel. After flash-chromatography (SiO_2-gel, 0.5 % EtOAc/hexanes) purification, bodipy's were obtained as a red crystals (0.0102 g, 79% yield); mp 146-148 °C; TLC (15% EtOAc/hexanes, R_f = 0.35); IR (KBr, cm-1): 3425 (w), 1724 (w), 1522 (m), 1500 (m), 1477 (m), 1457 (m), 1404 (s), 1391 (s), 1367 (s), 1279 (s), 1238 (m), 1197 (m), 1173 (s), 1173 (s), 1061 (s), 1007 (m), 967 (s), 828 (w), 747 (m), 710 (w); ^{1}H NMR (400 MHz, $CDCl_3$): δ= 7.56 (s, 1H), 7.25 (d, J = 4.0 Hz, 1H), 6.42 (d, J = 4.0 Hz, 1H), 2.70 (s, 3H), 2.55 (s, 3H), 2.52 (s, 3H); ^{13}C NMR (101 MHz, $CDCl_3$): δ= 155.4, 147.7, 140.8, 137.7, 132.9, 126.4, 115.8, 112.5, 21.5, 15.9, 13.1; HRMS (ESI+): *m/z* calcd. for $C_{12}H_{13}BBrF_2N_2S$ $[M+H]^+$, 345.0033; found 345.0033.

Photophysical properties.

Commercial Dyes. PM546 and PM567 were purchased from Exciton (laser grade), whereas BODIPY 505/515 from Invitrogen, and were used without further purification.

Spectroscopic Measurements. The photophysical properties were registered in diluted solutions (around 2×10^{-6} M) of tetrahydrofurane, using quartz cuvettes with optical pathway of 1 cm. UV-Vis absorption and fluorescence spectra were recorded on a Varian model CARY 4E spectrophotometer and a SPEX Fluorolog 3-22 spectrofluorimeter, respectively. Fluorescence quantum yield (ϕ) was obtained by using the commercial PM546 dye as reference (ϕ^r = 0.85 in ethanol). Radiative decay curves were registered with the time correlated single-photon counting technique (Edinburgh Instruments, model FL920), equipped with a microchannel plate detector (Hamamatsu C4878) of picosecond time-resolution (20 ps). Fluorescence emission was monitored at the maximum emission wavelength after excitation at 470 nm by means of a diode laser (PicoQuant, model LDH470) with 150 ps FWHM pulses. The fluorescence lifetime (τ) was obtained after the deconvolution of the instrumental response signal from the recorded decay curves by means of an iterative method. The goodness of the exponential fit was controlled by statistical parameters (chi-square, Durbin-Watson and the analysis of the residuals). Radiative (k_{fl}) and non-radiative (k_{nr}) rate constants were calculated as follows; $k_{fl} = \phi/\tau$ and $k_{nr} = (1-\phi)/\tau$.

Computational Simulations. Ground state energy minimizations were performed using the Becke´s Three Paramaters (B3LYP) Density Functional (DFT) method, whereas excited state geometry optimization was carried out using the Time Dependent (TD B3LYP) method. The basis set was the double valence 6-31+g* (with a diffuse and polarization function). The optimized geometry was taken as a true energy minimum using frequency calculations (no negative frequencies). Rotational energy barriers in the ground state were calculated from the potential energy surface, which was simulated by relaxed scans (steps of 10º) of the 8-phenyl, twist with regard to the plane of the dipyrrin core. The charge distribution was calculated by the CHelpG method. The solvent effect (tetrahydrofurane) was considered in all the calculations by the Polarizable Continuum Model (PCM). All the calculations were performed in Gaussian 09, using the "arina" computational resources provided by the UPV-EHU.

Acknowledgements

The authors thank CONACyT, Mexico (Grants 129572 and 123732), and MINECO (MAT2014-51937-C3-03) and Gobierno Vasco (IT912-16) of Spain for financial support. A. J. G-I. wishes to thank CONACyT for doctoral scholarship and I. V.-E. for postdoctoral fellowship. R. P. thanks UPV/EHU by a predoctoral fellowship.

Keywords: BODIPY dyes • synthesis • photophysics • structural effect • theoretical simulations

[1] For review papers, see: a) G. Ulrich, R. Ziessel, A. Harriman, *Angew. Chem. Int. Ed*. 2008, **47**, 1184-1201; b) A. Loudet, K. Burgess, *Chem. Rev*. 2007, **107**, 4891-4932; c) R. Ziessel, G. Ulrich, A. Harriman, *New J. Chem*. 2007, **31**, 496-501; d) Y. Ni, J. Wu, *Org. Biomol. Chem*. 2014, **12**, 3774-3791; e) H. Lu, J. Mack, Y. Yang, Z. Shen, *Chem. Soc. Rev*. 2014, **43**, 4778-4823; f) N. Boens, V. Leen, W. Dehaen, *Chem. Soc. Rev*. 2012, **41**, 1130-1172; g) T. Kowada, H. Maeda, K. Kikuchi, *Chem. Soc. Rev*. 2015, **44**, 4953-4972; h) V. Lakshmi, M. Rajeswara Rao, M. Ravikanth, *Org. Biomol. Chem*., 2015, **13**, 2501-2517. For recent applications see: a) D. Zhai, B. K. Agrawalla, P. S. Fronia Eng, S.-C. Lee, W. Xua, Y.-T. Chang, *Chem. Commun.,* 2013, **49**, 6170-6172; b) J. Fan, M. Hu, P. Zhan and X. Peng, *Chem. Soc. Rev*., 2013, **42**, 29-43: c) A. Kamkaew, S. H. Lim, H. B. Lee, L. V. Kiew, L. Y. Chung, K. Burgess, *Chem. Rev*. 2013, **42**, 77-80; d) D. Su, J. Oh, S.-C. Lee, J. M. Lim, S. Sahu, X. Yu, D. Kim, Y.-T. Chang, *Chem. Sci*., 2014, **5**, 4812–4818; e) S. Husen Alamudi, R. Satapathy, J. Kim, D. Su, H. Ren, R. Das, L. Hu, E. Alvarado-Martínez, J. Y. Lee, C. Hoppmann, E. Peña-Cabrera, H.-H. Ha, H.-S. Park, L. Wang, Y.-T. Chang, *Nat. Commun*., 2016, **7**, 11964.

[2] T. V. Goud, A. Tutar, J.-F. Biellmann, *Tetrahedron* 2006, **62**, 5084-5091.

[3] a) H. Prokopcová, C. O. Kappe, *Angew. Chem. Int. Ed*. 2008, **47**, 3674-3676; b) H. Prokopcová, C. O. Kappe*, Angew. Chem. Int. Ed*. 2009, **48**, 2276-2286.

[4] a) E. Peña-Cabrera, A. Aguilar-Aguilar, M. Gonzalez-Dominguez, E. Lager, R. Zamudio-Vazquez, J. Godoy-Vargas, F. Villanueva-García, *Org. Lett*. 2007, **9**, 3985-3988; b) L. Betancourt-Mendiola, I. Valois-Escamilla, T. Arbeloa, J. Bañuelos, I. López Arbeloa, J. O. Flores-Rizo, R. Hu, E. Lager, C. F. A. Gómez-Durán, J. L. Belmonte-Vázquez, M. Martínez-González, I. J. Arroyo, C. A. Osorio-Martínez, E. Alvarado-Martínez, A. Urías-Benavides, B. D. Gutiérrez-Ramos, B. Z. Tang, E. Peña-Cabrera, *J. Org. Chem*. 2015, **80**, 5771-5780.

[5] I. Esnal, A. Urías-Benavides, C. F. A. Gómez-Durán, C. A. Osorio-Martínez, I. García-Moreno, A. Costela, J. Bañuelos, N. Epelde, I. López Arbeloa, R. Hu, B. Z. Tang, E. Peña-Cabrera, *Chem. Asian J*. 2013, **8**, 2691-2700.

[6] R. I. Roacho, A. Metta-Magaña, E. Peña-Cabrera, K. H. Pannell, *Org. Biomol. Chem*. 2015, **13**, 995-999.

[7] J. O. Flores-Rizo, I. Esnal, C. A. Osorio-Martínez, C. F. A. Gómez-Durán, J. Bañuelos, I. López Arbeloa, K. H. Pannell, A. J. Metta-Magaña, E. Peña-Cabrera, *J. Org. Chem*. 2013, **78**, 5867-5877.

[8] B. D. Gutiérrez-Ramos, J. Bañuelos, T. Arbeloa, I. López Arbeloa, P. E. González-Navarro, K. Wrobel, L. Cerdán, I. García-Moreno, A. Costela, E. Peña-Cabrera, *Chem. Eur. J*. 2015, **21**, 1755-1764.

[9] I. Esnal, I. Valois-Escamilla, C. F. A. Gomez-Durán, A. Urias-Benavides, M. L. Betancourt-Mendiola, I. Lopez Arbeloa, J. Bañuelos, I. Garcia-Moreno, A. Costela E. Peña-Cabrera, *ChemPhysChem* 2013, **14**, 4134-4142.

[10] C. F. A. Gómez-Durán, I. Esnal, I. Valois-Escamilla, A. Urías-Benavides, J. Bañuelos, I. López Arbeloa, I. García-Moreno, E. Peña-Cabrera, *Chem. Eur. J*. 2016, **22**, 1048-1061.

[11] V. Lakshmi, R. Sharma, M. Ravikanth, *Reports in Organic Chemistry* 2016, **6**, 1-24.

[12] a) T. Bruhn, G. Pescitelli, S. Jurinovich, A. Schaumlöffel, F. Witterauf, J. Ahrens, M. Bröring, G. Bringmann, *Angew. Chem. Int. Ed*. 2014, **53**, 14592-14595; b) G. Beer, C. Niederalt, S. Grimme, J. Daub, *Angew. Chem. Int. Ed*. 2000, **39**, 3252-3255; c) S. Kolemen, Y. Cakmak, Z. Kostereli, E. U. Akkaya, *Org. Lett*. 2014, **16**, 660-663; d) E. M. Sánchez-Carnerero, F. Moreno, B. L. Maroto, A. R. Agarrabeitia, J. Bañuelos, T. Arbeloa, I. López-Arbeloa, M. J. Ortiz, S. de la Moya, *Chem. Commun*. 2013, **49**, 11641-11643; e) E. M. Sánchez-Carnerero, F. Moreno, B. L. Maroto, A. R. Agarrabeitia, M. J. Ortiz, B. G. Vo, G. Muller, S. de la Moya, *J. Am. Chem. Soc*. 2014, **136**, 3346-3349; f) H. Lu, J. Mack, T. Nyokong, N. Kobayashi, Z. Shen, *Coord., Chem. Rev*., 2016, **318**, 1-15.

[13] a) J. Ahrens, B. Haberlag, A. Scheja, M. Tamm, M. Bröring, *Chem. Eur. J*. 2014, **20**, 2901-2912; b) S. Rihn, M. Erdem, A. De Nicola, P. Retailleau, R. Ziessel, *Org. Lett*. 2011, **13**, 1916-1919; c) A. C. Benniston, G. Copley, A. Harriman, D. Howgego, R. W. Harrington, W. Clegg, *J. Org. Chem.*, 2010, **75**, 2018–2027; d) L. Gai, H. Lu, B. Zou, G. Lai, Z. Shen, Z. Li *RSC Advances,* 2012, **2**, 8840–8846.

[14] I. J. Arroyo, R. Hu, G. Merino, B. Z. Tang, E. Peña-Cabrera, *J. Org. Chem*. 2009, **74**, 5719-5722.

[15] a) A. Cui, X. Peng, J. Fan, X. Chen, Y. Wu, B. Guo, *J. Photochem. Photobiol. A* 2007, **186**, 85-92; b) S. Mukherjee, P. Thilagar, *RSC Adv*. 2015, **5**, 2706-2714.

[16] P. G. Wadell, X. Liu, T. Zhao, J. M. Cole, Dyes and Pigments 2015, 116, 74-81.

[17] J. Bañuelos, A. R. Agarrabeitia, I. García-Moreno, I. López-Arbeloa, A. Costela, L. Infantes, M. E. Pérez-Ojeda, M. Palacios-Cuesta, M. J. Ortiz, *Chem. Eur. J*. 2010, **16**, 14094-14105.

[18] a) F. Li, S. I. Yang, Y. Ciringh, J. Seth, C. H. Martin III, D. L. Singh, D. Kim, R. R. Birge, D. F. Bocian, D. Holten and J. S. Lindsey, *J. Am. Chem. Soc*. 1998, **120**, 10001-10017; b) H. L. Kee, C. Kirmaier, L. Yu, P. Thamyongkit, W. J. Youngblood, M. E. Calder, L. Ramos, B. C. Noll, D. F. Bocian, W. R. Scheidt, R. R. Birge, J. S. Lindsey, D. Holten, *J. Phys. Chem. B* 2005, **109**, 20433-20443; c) M. A. H. Alamiry, A. C. Benniston, G. Copley, K. J. Elliott, A. Harriman, B. Stewart, Y.-G. Zhi, *Chem. Mater*. 2008, **20**, 4024-4032; d) M. K. Kuimova, G. Yahioglu, J. A. Levitt, K. Suhling, *J. Am. Chem. Soc*. 2008, **130**, 6672-6673.

[19] a) J. Chen, A. Burghart, A. Derecskei-Kovacs, K. Burgess, *J. Org. Chem.* 2000, **65**, 2900-2906; b) Q. Zheng, G. Xu, P. N. Prasad, *Chem. Eur. J*. 2008, **14**, 5812-5819.

[20] W. Qin, M. Baruah, M. Van der Auweraer, F. C. De Schryver, N. Boens, *J. Phys. Chem. A* 2005, **109**, 7371-7384.

[21] M. Kollmannsberger, K. Rurack, U. Resch-Genger, J. Daub, *J. Phys. Chem. A* 1998, **102**, 10211-10220.

[22] Z. R. Grabowski, K. Rotkiewicz, W. Rettig, *Chem. Rev*. 2003, **103**, 3899-4032.

[23] H. E. Gottlieb, V. Kotlyar, A. Nudelman, *J. Org. Chem*. 1997, **62**, 7512-7515.

[24] S. Zhang, D. Zhang, L. S. Liebeskind, *J. Org. Chem*. 1997, **62**, 2312-2313. CuTC is also commercially available.

Entry for the Table of Contents

FULL PAPER

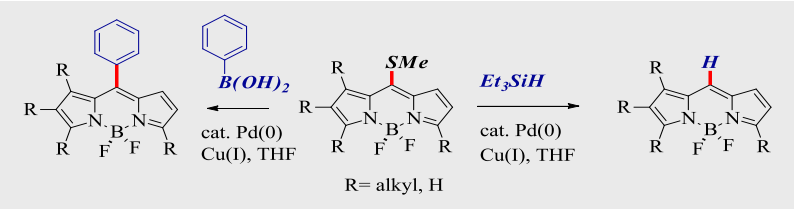

Novel non-symmetric 8-methylthioBODIPYs with selective alkylation of the pyrroles, were straigthforwardly synthesized. From these priviledge scaffolds specific functionalization at *meso* position was afforded. The combined photophysical and computational characterization of these dyes provides key structural guidelines to modulate their spectral bands positions as well as their fluorescence response.

Tailor-made BODIPYs

A. J. Gómez-Infante, J. Bañuelos, I. Valois-Escamilla, D. Cruz-Cruz, R. Prieto-Montero, I. López-Arbeloa, T. Arbeloa, E. Peña-Cabrera**

Page No. – Page No.

Synthesis, Properties, and Functionalization of Non-symmetric ~~Biellmann~~ 8-methylthioBODIPYs